

# Numerical analysis of ground plane size effects on patch array antenna characteristics for mobile satellite communications

Josaphat Tetuko Sri Sumantyo<sup>1,2,\*;†,‡</sup>, Koichi Ito<sup>3</sup>, David Delaune<sup>4</sup>,  
Toshimitsu Tanaka<sup>4</sup>, Teruo Onishi<sup>4</sup> and Hiroyuki Yoshimura<sup>5</sup>

<sup>1</sup>Center for Frontier Electronics and Photonics, Chiba University, Japan

<sup>2</sup>Remote Sensing Research Center, Pandhito Panji Foundation, Jalan Ligar Raya 52B, Bukit Ligar, Bandung 40191, Indonesia

<sup>3</sup>Research Center for Frontier Medical Engineering, Chiba University, Japan

<sup>4</sup>Graduate School of Science and Technology, Chiba University, Japan

<sup>5</sup>Department of Urban Environment Systems, Faculty of Engineering, Chiba University, 1-33 Yayoi, Inage, Chiba 263-8522, Japan

## SUMMARY

In this research, a patch array antenna for mobile satellite communications aiming at ETS-VIII applications has been developed. The ground plane size effects on the antenna characteristics were investigated. Finite and infinite ground planes were analysed by the finite integration technique (FIT) for time domain analysis, the finite element method (FEM) and the method of moments (MoM) for spectral domain analysis. Then measurements of the fabricated antenna were performed to confirm the analysis results. It is clear that the frequency characteristics of the axial ratio are influenced by the variation in the ground plane size. When the ground plane size is increased, the edge-diffracted field causes tilting of the beam in the direction of low elevation angles and causes a decrease in the maximum gain and in the 3 dB-beamwidth of axial ratio in the elevation plane. In the conical-cut direction, an increase in ground plane size induces a decrease in the 3 dB-beamwidth of axial ratio for FEM, but shows the opposite result for FIT and measurement. In addition, an increase in ground plane size also induces increases in maximum gain and its 6 dBic-beamwidth along with a shift in the maximum gain in the direction of low azimuth angle. Copyright © 2004 John Wiley & Sons, Ltd.

KEY WORDS: MoM; FIT; FEM; ground plane size; ETS-VIII; patch array antenna

## 1. INTRODUCTION

The Japan Aerospace Exploration Agency (JAXA) will launch a geostationary satellite called Engineering Test Satellite-VIII (ETS-VII) in 2005. ETS-VIII will conduct orbital experiments on

\*Correspondence to: J. T. Sri Sumantyo, Remote Sensing Research Centre, Pandhito Panji Foundation, Jalan Ligar Raya 52B, Bukit Ligar, Bandung 40191, Indonesia.

†E-mail: tetuko@pandhitopanji-f.org

‡E-mail: tetuko@restaff.chiba-u.jp

mobile satellite communications at the S-band frequency, especially to support the development of a technology for the transmission and reception of multimedia information such as voice and images for land mobile systems [1].

Up to now, various antennas have been developed for mobile satellite communications purposes [2–5], but these antennas have a complex composition and bulky structures. Hence, in this research, a simple satellite-tracking four elements left-handed circularly polarized (LHCP) stacked patches microstrip array antenna is proposed. The targeted minimum gain of the antenna is set to 6 dBic at an elevation of  $48^\circ$  in Tokyo area for applications of a few hundred kbps data transfer. Here dBic is used to define the gain of the antenna system relative to an isotropic radiator of circular polarization. The antenna should be as small and simple as possible, because it will be mounted on bullet train, ship and car roofs. Actually, the roof is made of metal and its size is greater than the antenna size [6]. Hence an antenna with a large ground plane should be considered. Thus, in this paper, the effects of the ground plane size will be discussed.

Section 2 introduces the antenna specifications, targets and configuration. Then the methods used to analyse the antenna are shown in Section 3. The characteristics are numerically investigated for two cases of antennas: a finite and an infinite size of ground plane, respectively. Those results are discussed in Section 4. Finally, the conclusions and recommendations are summarized in Section 5.

## 2. ANTENNA SPECIFICATIONS, TARGETS AND CONFIGURATION

Table I shows the specifications and targets of the antenna for mobile satellite communications aiming at ETS-VIII applications that are used in this research. Here, a thin miniaturized antenna designed for a few hundred kbps data transfer is considered. In addition, the measurements will take place in the centre of Tokyo. As a result, the targeted elevation angle  $E_l$  is set to  $48^\circ$  [1].

In this research, the operating frequency is fixed at 2.50 GHz (for reception). The antenna is fabricated using a conventional substrate (relative permittivity: 2.17) and measured to confirm the analysis results. Figure 1 shows the composition of the patch array antenna that is made of four elements with the parasitic patches (a) and the radiating patches (b), where this configuration is used to increase the gain. The sizes of radiating and parasitic patches are optimized to obtain the resonance frequency at 2.50 GHz. The side view of the antenna is shown

Table I. Specifications and targets of the antenna mobile satellite communications.

<i>Specifications</i>		
Frequency bands	Transmission (TX)	2655.5–2658.0 MHz
	Reception (RX)	2500.5–2503.0 MHz
Polarization	Left-handed circular polarization for both TX and PX	
<i>Targets</i>		
Angular ranges	Elevation angle (EL)	$48^\circ$ (Tokyo)
	Azimuth angle (Az)	$0\text{--}360^\circ$
	Minimum gain	6 dBic
	Maximum axial ratio	3 dB

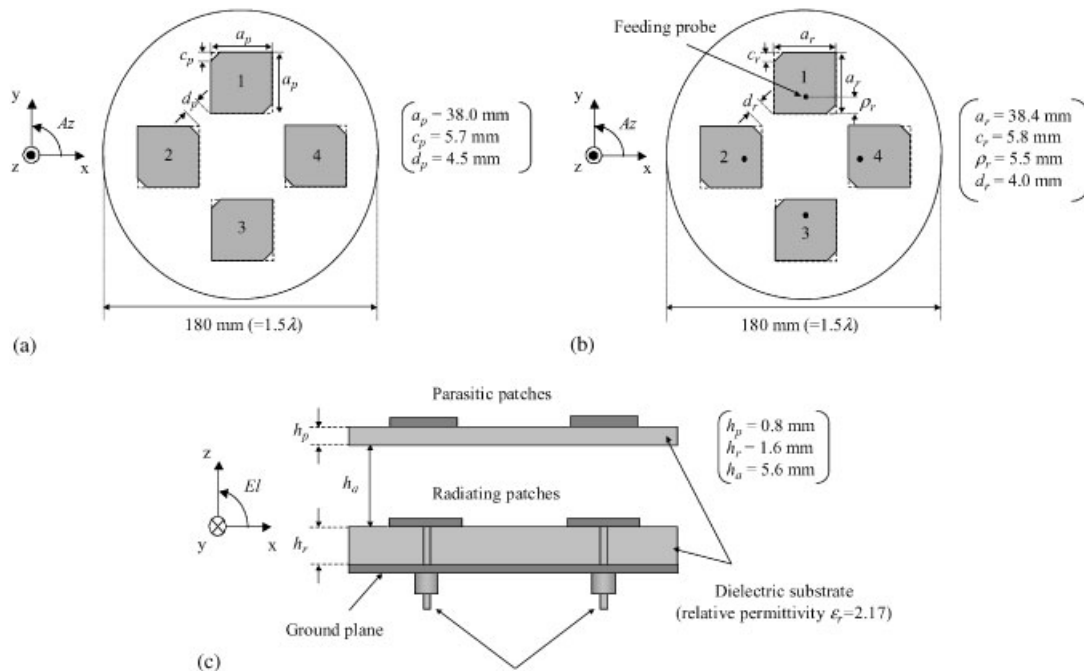


Figure 1. Antenna configuration: (a) parasitic patches, (b) radiating patches, (c) side view.

in Figure 1(c). Figure 2 shows the fabricated antenna. Figure 3 represents the analysis model with a substrate diameter  $s$  for both parasitic and radiating patches array equal to  $180\text{ mm}$  ( $s = 1.5\lambda$ ).

The beam of the antenna is generated by a simple mechanism that consists in switching OFF one of the radiating elements shown in Figure 1(b). By considering the mutual coupling between fed elements, their phases and distances, the beam direction can be varied [7,8]. Hence, the three fed elements generate a beam shifted  $-90^\circ$  in the conical-cut direction from the element which is turned OFF, in the case of an LHCP antenna. For example, when element 4 is OFF, the beam is directed towards the azimuth angle  $Az = 270^\circ$ . In the same manner, the other three beams can be generated by successively switching OFF each element. In this paper, the antenna characteristics will be discussed only when element 4 is OFF.

### 3. ANALYSIS METHODS

The method of moments (MoM) is assessed to analyse the antenna with an infinite ground plane and substrate. The software used was Ensemble™ version 8 (Ansoft). Then the finite element method (FEM) was applied to analyse the finite substrate (refer to Figures 1 and 3) with a diameter  $s = 1.5\lambda$  and a circular finite ground plane with a diameter  $1.5\lambda$  (code in figure: FEMC). Due to the computer memory capacity and aiming at examining the ground plane size

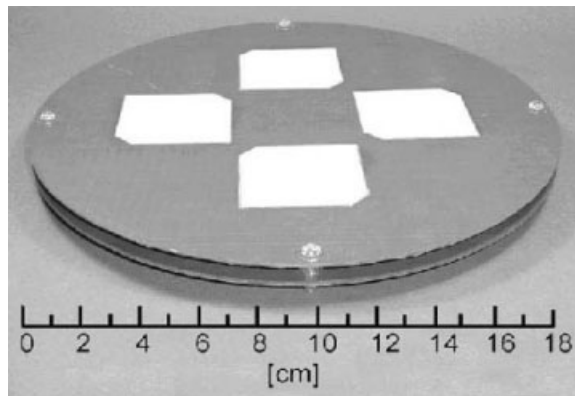


Figure 2. Fabricated antenna.

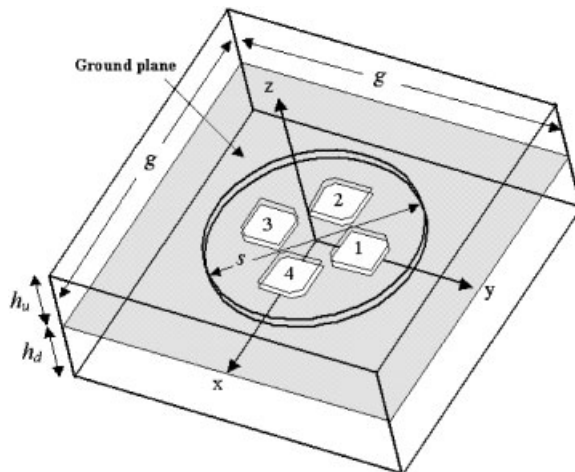


Figure 3. Analysis model.

effects, finite substrates with the same diameter as before, but with ground planes whose sizes are  $g = 2.0\lambda$ ,  $2.5\lambda$ ,  $3.0\lambda$  and  $3.5\lambda$  (code in figure: FEM1, FEM2, FEM3, and FEM4, respectively) were investigated. These ground plane sizes (larger than  $\lambda$ ) are enough to diminish the ripples or scalloping in the main pattern due to the interferences from the fields diffracted from the edges of the ground plane, as mentioned in References [9,10]. The analysis spaces above and under the antenna are both set to  $h_u = h_d = 0.5\lambda$ . The influence of the boundary conditions on the extremities of the ground plane was not considered here. The FEM used the software HFSS<sup>TM</sup> (Ansoft). The time domain analysis employed the finite integration technique (FIT) to analyse the ground plane effects with the same model as the one analysed by FEM (code in figure: FITC, FIT1, FIT2, FIT3, and FIT4). The FIT utilizes the software MW-Studio version 4 (CST

GmbH). Then an antenna with the same size as presented above, was fabricated and measured to confirm the analysis results (code in figure: MC, M1, M2, M3, and M4).

The analysis runtimes of MoM, FEMC, FEM1, FEM2, FEM3, and FEM4 are 0.6, 4.2, 5.3, 5.6, 4.9, and 10.1 h, respectively. Then FITC, FIT1, FIT2, FIT3, and FIT4 are 5.8, 2.5, 2.9, 3.9, and 5.8 h, respectively. The runtime of FITC is longer than the ones of FIT1 to FIT3, because the mesh modelling of the ground plane in the former case is denser (circular shape) than the others (square shape). The computers used were a Celeron™, 1.1 GHz, 1.0 GB RAM for MoM, and an Athlon™, 1.2 GHz, 1.5 GB RAM for FIT and FEM. The same antenna parameters were used for the three methods, namely MoM, FIT and FEM, because the goal of this research was to compare the same model with different methods.

In this research, as a result of the analysis runtime and the time efficiency explained in the previous paragraph, and by considering the real condition of the antenna when installed on the car roof, the MoM is used as the reference to design the antenna with an infinite ground plane to meet the specifications. The parameters are shown in Figure 1. Then, an antenna with various ground sizes was measured in the radio anechoic chamber of the Graduate School of Science and Technology, Chiba University, Japan.

#### 4. RESULTS AND DISCUSSION

At first, the performance of each antenna model is analysed in terms of axial ratio characteristics. Up to now, numerical and analytical techniques have been used to analyse the characteristics of linearly polarized single element antennas with infinite and finite ground planes [9–14]. Here, the characteristics of a circularly polarized array antenna are analysed to find out which differences can occur as compared to the previous case. Figure 4 depicts the relationship between the axial ratio and the frequency for numerical analysis as well as the measurement results for  $Az = 270^\circ$  and  $EI = 48^\circ$  (element 4 OFF). Figure 4(a) shows that the frequency characteristics of the finite ground plane analysed by FEM (FEMC), FIT (FITC) and measurement (MC) are, respectively, shifted of 40, 60 and 20 MHz to the low frequencies compared to the MoM (2.50 GHz). Then Figures 4(b)–4(d) show that the model with the largest ground plane analysed by FEM (FEM4) and the measurement (M4) result satisfy the specification, but for FIT (FIT4) it is still shifted of 40 MHz. As a result of this research, it is shown that the ground plane size also influences the characteristics of a circularly polarized patch array antenna as can be seen in the axial ratio characteristics, where the antenna characteristics of each model and measurement are considered at each respective frequency of minimum axial ratio. This result also shows that the frequency characteristics of axial ratio are sensitively influenced by the ground plane size.

Previous reports explained that the finite ground plane gives rise to diffraction from the edges of the ground plane resulting in changes in radiation pattern and resonant frequency of single element antenna [15–19]. This effect also changes the performance of the antenna in the elevation plane and in the conical-cut direction in the case of a circularly polarized patch array antenna as explained after in detail. In this section, the verification of analysis and measurement results is expressed by comparing them to the MoM result that presents conditions close to the real antenna mounted on the car roof. With this method, the antenna characteristics, the input impedance etc, are very well predicted from the infinite ground plane model [16].

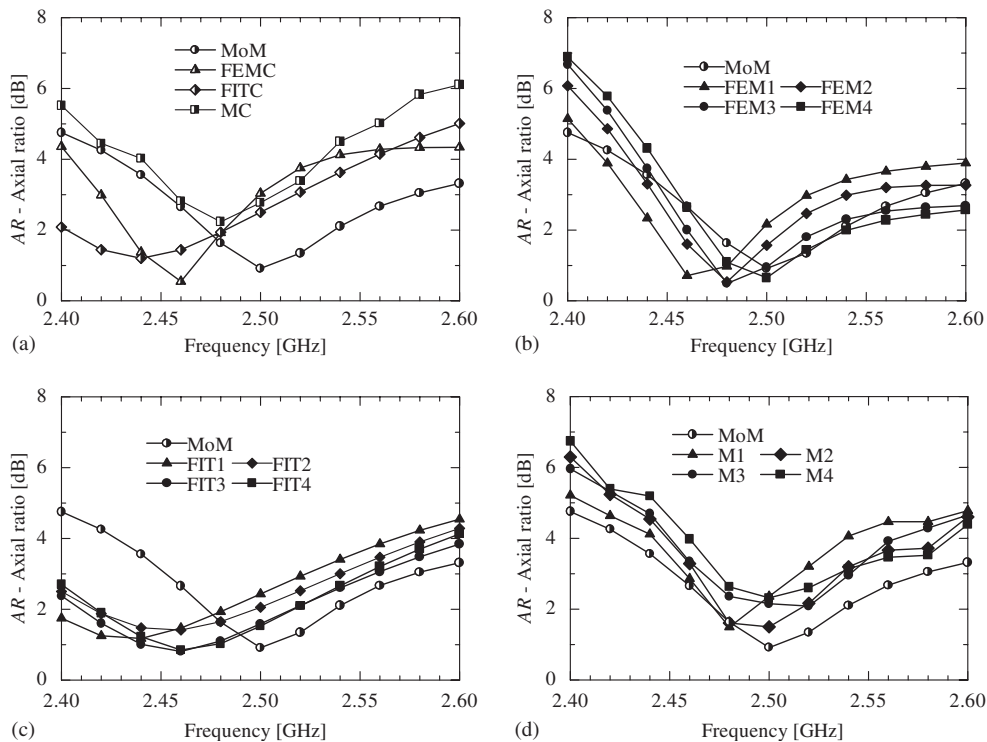


Figure 4. Relationship between axial ratio and frequency: (a) MoM (infinite ground plane), FEM, FIT and measurement (finite circular ground plane), (b) MoM and FEM, (c) MoM and FIT, (d) MoM and measurement.

Figure 5 shows the relationship between the  $S$  parameters ( $S_{11}$ ) and the frequency of each model. From Figure 5(a), the frequency characteristics of finite ground plane analysed by FEM (FEMC), FIT (FITC) and measurement (MC) are shifted of 40, 60 and 20 MHz to the low frequencies compared to the MoM (2.60 GHz). Figures 5(b)–5(d) show that the minimum  $S_{11}$  of FEM, FIT and measurement results are shifted of 50, 60 and 25 MHz from MoM (2.60 GHz), and that an increase in the ground plane size improves the performances of  $S_{11}$ .

Figure 6 depicts the relationship between the gain  $G$  and the elevation angle  $EI$  while Figure 7 shows the relationship between the beam direction and the ground plane size in the elevation plane. In Figure 6(a) the gain obtained by MoM and FIT analysis is shown in the elevation plane. From this figure, the maximum gain obtained by MoM is lower than FIT. An increasing ground size induces a decrease in the elevation angle of maximum gain. The effect of ground plane size on the radiated field of a single element has been studied [9,10,15], and it was shown that it affects strongly the E-plane radiation pattern. Therefore, it is considered to influence the switched radiation pattern in the array antenna and to tilt the beam direction to low elevation angle. Colburn *et al.* reported the same result that the ground plane size affects the radiation characteristics of a single element, especially in elevation angle  $EI$  about  $45^\circ$  [20]. Figures 6(b) and 6(c) show the same result for FEM and measurement (see Figure 7 for summary). From Figures 6(a)–6(c), the direction of maximum gain is almost the same in terms of elevation for

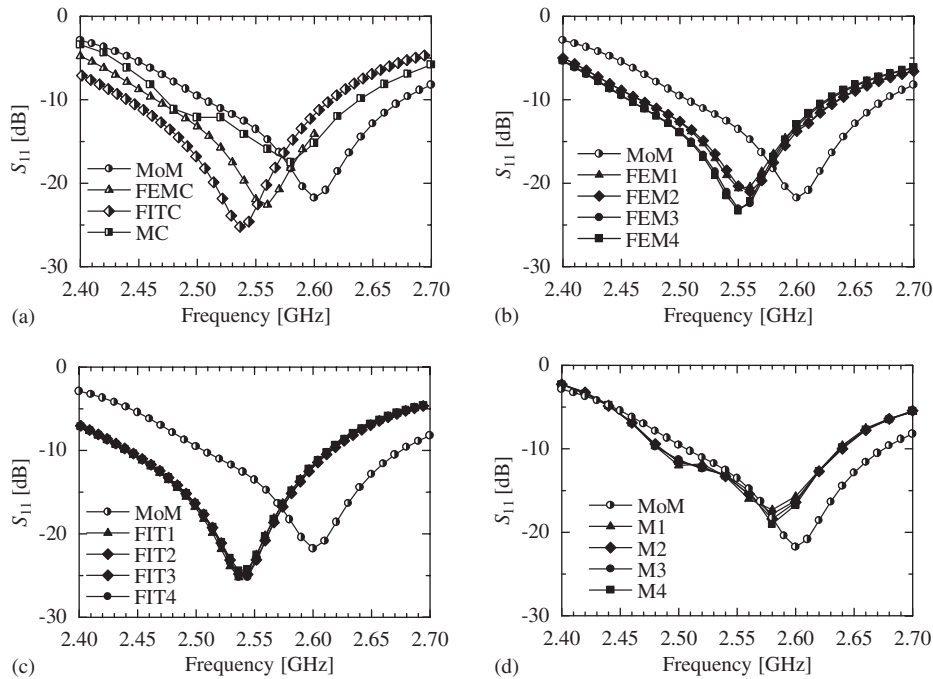


Figure 5. Relationship between  $S_{11}$  and frequency: (a) MoM (infinite ground plane), FEM, FIT and measurement (finite circular ground plane), (b) MoM and FEM, (c) MoM and FIT, (d) MoM and measurement.

FIT, FEM and measurement. Figure 6(c) shows that the maximum gain of MoM is lower than for measurement (MC), and its elevation angle is the same as for M4 and tilted of  $4^\circ$  in the direction of low elevation angle for MC. It is due to the same reason [9] as shown in Figures 6(a) and 6(b), especially when the measured antenna and the MoM model have a finite and an infinite ground plane, respectively.

Figure 8 summarizes the relationship between maximum gain and ground plane size of FEM and FIT analysis and measurement in the elevation plane (FEM-EL, FIT-EL, measurement-EL) and in the conical-cut direction (FEM-AZ, FIT-AZ, measurement-AZ), where the conical-cut result will be discussed later. This figure shows that an increase in ground size from  $g = 2.0\lambda$  to  $3.5\lambda$  induces a decrease in maximum gain in the elevation plane. Note that this result does not occur at  $g = 1.5\lambda$ .

Figure 9 shows the relationship between the axial ratio AR and EI in the elevation plane. From Figures 9(a)–9(c), the 3 dB-beamwidth of axial ratio of MoM is wider than FIT and FEM, and is narrower than measurement. The figure also shows that an increase in ground plane size induces a decrease in the 3 dB-beamwidth for the elevation plane in the analyses and measurement. This phenomenon shows that an increase in ground plane size induces the edge effect that will affect the current distribution on the surface of the patches, therefore decreasing the axial ratio performance.

The relationship between azimuth angle Az and gain (conical-cut direction) is seen in Figure 10. This figure shows that maximum gain of MoM is lower than FIT, FEM, and

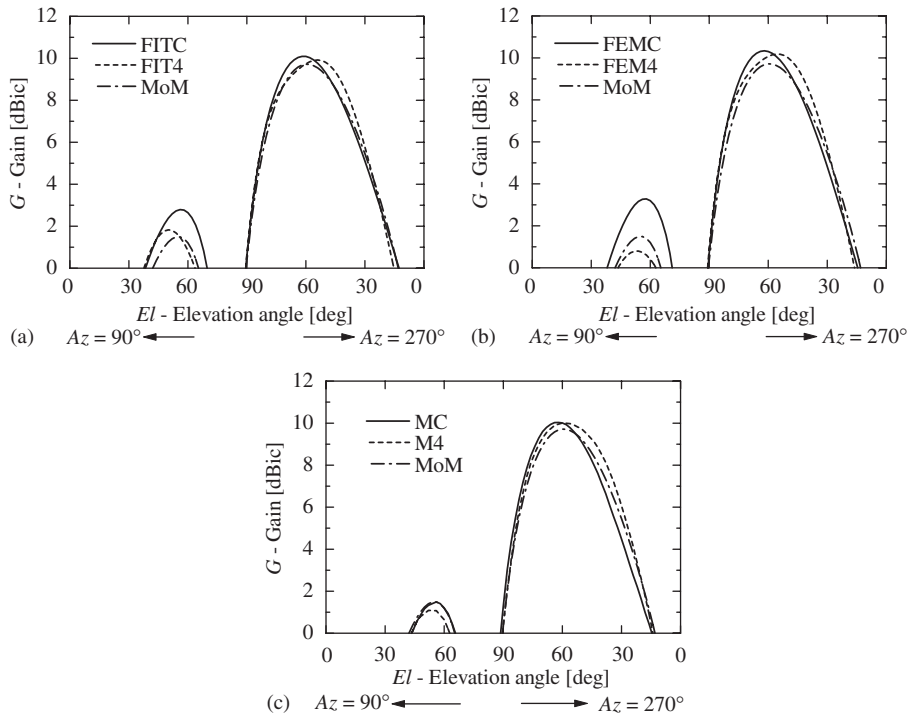


Figure 6. Relationship between gain and elevation angle (element 4 OFF): (a) MoM and FIT, (b) MoM and FEM, (c) MoM and measurement.

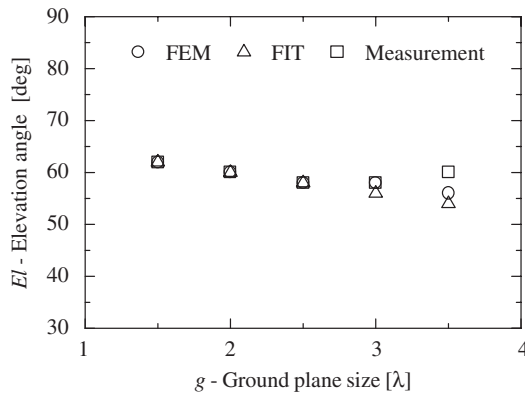


Figure 7. Relationship between beam direction in the elevation plane and ground plane size.

measurement, whose ground plane size is  $3.5\lambda$ . The figure also shows an increasing ground plane size induces an increase in the 6dBic-beamwidth of FIT and FEM, but a decrease in measurement. In Figures 10(a)–10(c), analysis results and measurement show that an increasing ground plane size induces an increase in maximum gain and shifts the azimuth angle to the low direction (refer to Figure 8). It is considered that an increase in the ground plane size induces a



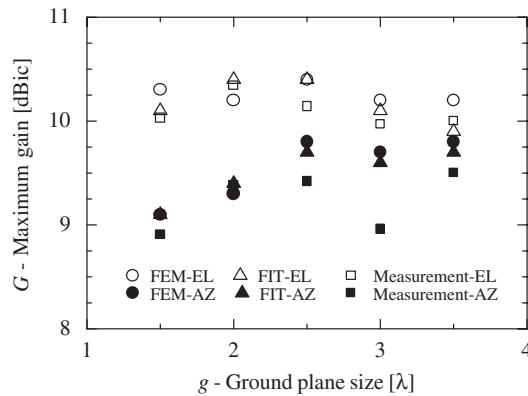


Figure 8. Relationship between maximum gain and ground plane size.

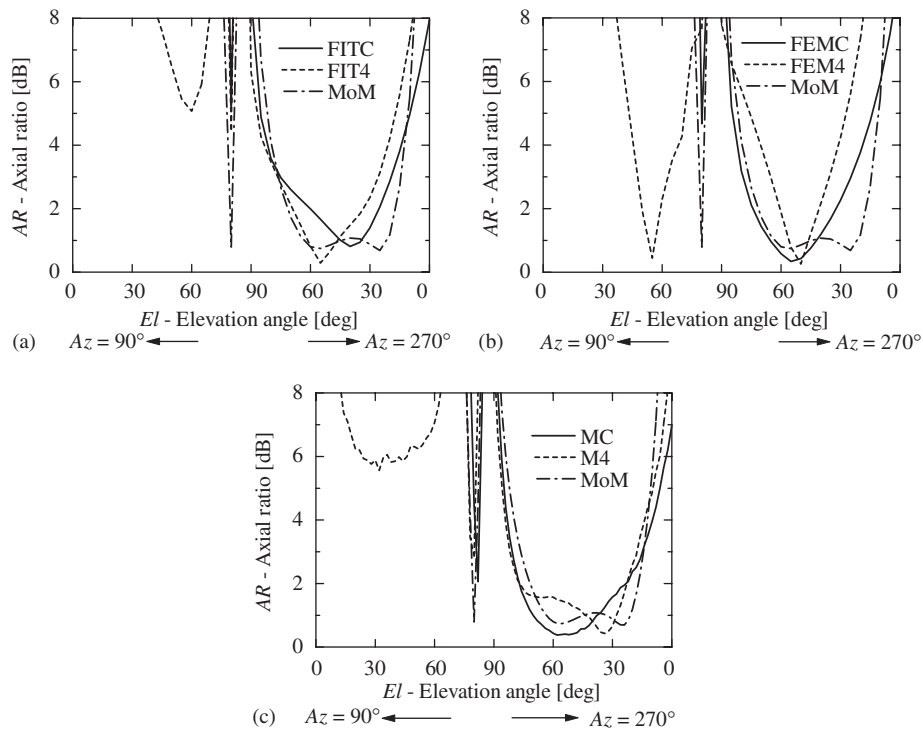


Figure 9. Relationship between axial ratio and elevation angle (element 4 OFF): (a) MoM and FIT, (b) MoM and FEM, (c) MoM and measurement.

stronger coupling between each active patch, therefore the main beam is shifted to low azimuth angle (refer to Figure 10). The maximum gain and the 6 dBic-beamwidth of FIT and FEM are almost the same. FIT, FEM and measurement satisfy the conditions that require the beam of the antenna to cover an azimuth range larger than 90°.

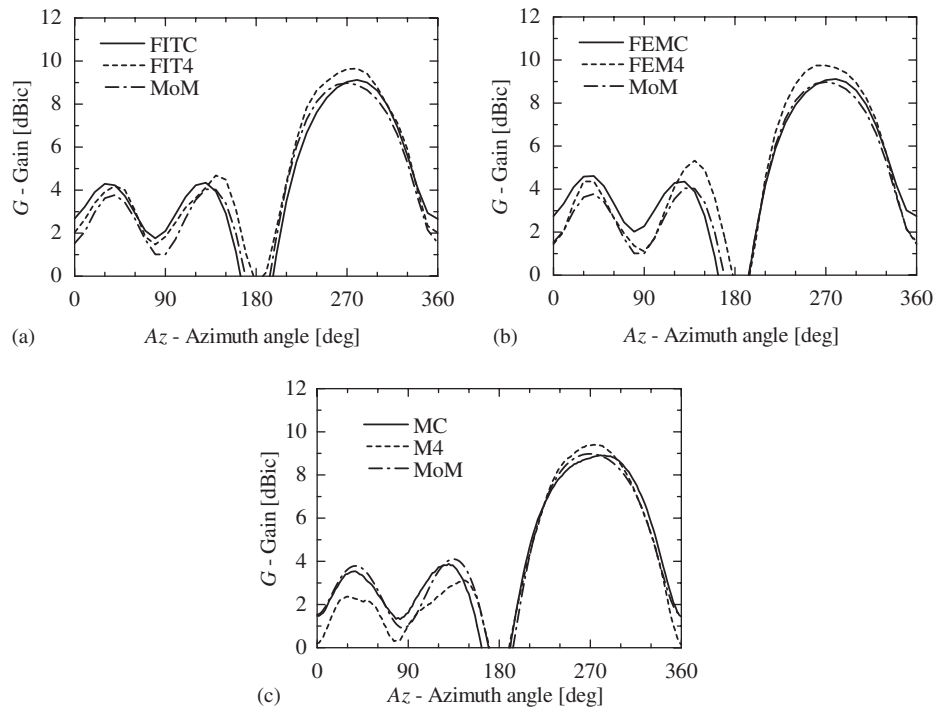


Figure 10. Relationship between gain and azimuth angle in the conical-cut direction (element 4 OFF) ( $EI = 48^\circ$ ): (a) MoM and FIT, (b) MoM and FEM, (c) MoM and measurement.

Figure 11 shows the relationship between AR and Az in the conical-cut direction. The beamwidth of MoM when AR is less than 3 dB is larger than for FIT and FEM, but smaller than for measurements. Figure 11(b) shows an increasing ground plane size induces a decrease in the 3 dB-beamwidth of FEM, but from Figures 11(a) and 11(c) the FIT and measurement show the opposite result. From these figures, the 3 dB-beamwidth of axial ratio satisfies the condition for the beam switching in the conical-cut direction because it is larger than  $90^\circ$ . Here, the edge effect will interfere with the current distribution on the surface of the patch, therefore it affects the axial ratio performance.

## 5. CONCLUSIONS

The ground plane size effects on a patch array antenna characteristics for mobile satellite communications aiming at ETS-VIII applications were investigated by use of the MoM, the FEM, and the FIT. Finite and infinite ground planes were analysed by the FIT for time domain analysis, the FEM and the MoM for spectral domain analysis. Then measurements of the fabricated antenna were performed to confirm the analysis results.

At first, the MoM was applied for numerical simulations. Then this result was used to design and fabricate the antenna. The analysis and measurement results show the frequency of

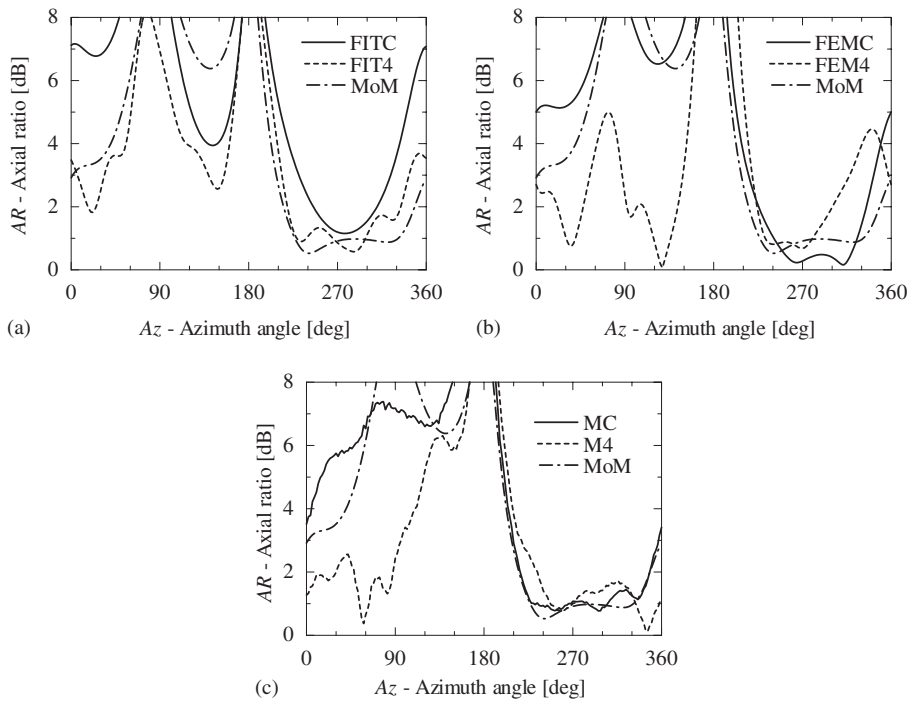


Figure 11. Relationship between axial ratio and azimuth angle in the conical-cut direction (element 4 OFF) ( $\theta = 48^\circ$ ): (a) MoM and FIT, (b) MoM and FEM, (c) MoM and Measurement.

minimum axial ratio is shifted towards the higher frequencies with an increase in the ground plane size. Then the frequency characteristics of minimum axial ratio were applied to each analysis model and measurement to determine the characteristics of ground plane size effects.

The analysis results and measurements show that an increasing ground plane size induces a tilting beam in the direction of low elevation angle and a decrease in maximum gain. A decrease in the 3 dB-beamwidth of axial ratio for the elevation plane is also observed. Regarding the conical-cut direction, it is shown that an increasing ground plane size induces an increase in maximum gain and shifts the azimuth angle to lower values. The mechanism of the effects described above can be explained by edge-diffracted fields. This effect influences the current distribution on the surface of patches, therefore affects the performance of gain and axial ratio.

The results discussed in this paper show that the characteristics of analysis model and fabricated antenna satisfy the specifications for ETS-VIII applications, although the beams of gain and axial ratio are shifted in both conical-cut direction and elevation plane. The relationship between ground plane size and the coupling effects between each patch in the array contributes to the shifted beam in the conical-cut direction.

By considering the results shown in Figures 4–11, we conclude that the MoM result is the closest to the measurement. The analysis with FIT and FEM was done without optimization of mesh or tetrahedral size in modelling, therefore it is recommended to optimize the size to obtain

a current distribution on the patch similar to the real phenomenon on each element surface to improve the antenna characteristics, especially the axial ratio.

The ground plane size influences the antenna characteristics, especially its axial ratio. Therefore, it is recommended to apply absorbent and resistive edge loading or lossy materials in the vicinity of the edges to minimize the diffracted fields [15,21].

#### ACKNOWLEDGEMENTS

The authors wish to acknowledge Dr Tanaka M, Dr Fujino Y, Dr Miura A, Dr Yamamoto S (Communications Research Laboratory), and Dr Saito K (Chiba University) for their valuable opinions. Prof. Uematsu T and Ms Komai Y (Chiba University) for their supports in this research.

#### REFERENCES

1. Jang J, Tanaka M, Hamamoto N. Portable and deployable antenna for ETS-VIII. *2002 Interim International Symposium on Antenna and Propagation*, Yokosuka, Japan, 2002; 49–52.
2. Ito K, Ohmaru K, Konishi Y. Planar antennas for satellite reception. *IEEE Transactions on Broadcasting* 1988; **34**(4):457–464.
3. Ito K, Daniel JP, Lenormand JN. A printed antenna composed of strip dipoles and slots generating circularly polarised conical patterns. *IEEE Antennas and Propagation International Symposium*, San Jose, USA, 1989; 632–635.
4. Fujimoto K, James J (eds). *Mobile Antenna Systems Handbook*. Artech House: Boston, London, 2001; 426–481.
5. Nakano M, Arai H, Chujo W, Fujise M, Goto N. Feed circuits of double-layered self-diplexing antenna for mobile satellite communications. *IEEE Transactions on Antennas and Propagation* 1992; **40**(10):1269–1271.
6. Ishihara H, Yamamoto A, Ogawa K. A simple model for calculating the radiation patterns of antennas mounted on a vehicle roof. *2002 Interim International Symposium on Antenna and Propagation*, Yokosuka, Japan, 2002; 548–551.
7. Ito K, Tanaka T, Delaune D, Onishi T, SS Tetuko J. Simple tracking stacked microstrip antenna. *IEE 2003 International Conference on Antennas and Propagations*, Exeter, UK, 2003; 389–392.
8. Delaune D, Tanaka T, Onishi T, SS Tetuko J, Ito K. Study on a simple satellite tracking on-board stacked antenna for ETS-VIII applications. *IEICE Technical Report*, AP2002(116), 2002; 25–30.
9. Huang J. The finite ground plane effect on the microstrip antenna radiation patterns. *IEEE Transactions on Antennas and Propagation* 1983; **31**(4):649–653.
10. Garg R, Bhartia P, Bahl I, Ittipiboon A. *Microstrip Antenna Design Handbook*. Artech House: Boston, London, 2001; 293–296.
11. Lier E, Jacobsen K. Rectangular microstrip patch antennas with infinite and finite ground plane dimensions. *IEEE Transactions on Antennas and Propagation* 1983; **31**(6):978–984.
12. Bokhari S, Mosig J, Gardiol F. Radiation pattern computation of microstrip antennas on finite size ground plane. *Proceedings of IEE* 1992; **139**(Part H):278–286.
13. Delgado H, Williams J, Long S. Antenna pattern measurement techniques for infinite ground plane simulation. *IEEE Antennas and Propagation International Symposium*, San Jose, USA, 1989; 339–342.
14. Williams J, Delgado H, Long S. An antenna pattern measurement technique for eliminating the fields scattered from the edges of a finite ground plane. *IEEE Transactions on Antennas and Propagation* 1990; **38**(11):1815–1822.
15. Otero M, Rojas R. Analysis and treatment of edge effects on the radiation pattern of a microstrip patch antenna. *IEEE Antennas and Propagation International Symposium*, New Port Beach, USA, 1995; 1050–1053.
16. Delgado H, Williams J, Long S. Subtraction of edge-diffracted fields in antenna radiation pattern for simulation of infinite ground plane. *Electronics Letters* 1989; **25**(11):694–696.
17. Iyer S, Karekar R. Edge effects for resonance frequency of covered rectangular microstrip patch antenna. *Electronics Letters* 1991; **27**(17):1509–1511.
18. Maci S, Borselli L. Diffraction at the edge of a truncated grounded dielectric slab. *IEEE Transactions on Antennas and Propagation* 1996; **44**(6):863–873.
19. Maci S, Borselli L, Cucurachi A. Diffraction from a truncated grounded dielectric slab: a comparative full-wave/physical-optics analysis. *IEEE Transactions on Antennas and Propagation* 2000; **48**(1):48–57.
20. Colburn J, Rahmat-Samii Y. Patch antennas on externally perforated high dielectric constant substrates. *IEEE Transactions on Antennas and Propagation* 1999; **47**(12):1785–1794.
21. Wang R, Liepa V. Reduction of the edge diffraction of a circular ground plane by using resistive edge loading. *IEEE Antennas and Propagation International Symposium*, Vancouver, Canada, 1985; 769–771.